The EMBO Journal vol.15 no.1 pp.23–33, 1996

Genetic variation of the poliovirus genome with two VPg coding units

Xuemei Cao and Eckard Wimmer

Department of Molecular Genetics and Microbiology, School of Medicine, State University of New York at Stony Brook, Stony Brook, NY 11794, USA

Amongst the picornaviruses, poliovirus encodes a single copy of the genome-linked protein, VPg, whereas foot-and-mouth disease virus uniquely encodes three copies of VPg. We have previously shown that a genetically engineered poliovirus genome containing two tandemly arranged VPgs is quasi-infectious (*qi*) that, upon genome replication, inadvertently deleted one complete VPg sequence. Using two genetically marked viral genomes with two VPg sequences, we now provide evidence that this deletion occurs via homologous recombination. The mechanism was abrogated when the second VPg was engineered such that its nucleotide sequence differed from that of the first VPg sequence by 36%. Such genomes also expressed a *qi* phenotype, but progeny viruses resulted from (i) random deletions yielding single VPg coding sequences of varying length lacking the Q*G cleavage site between the VPgs and (ii) mutations in the AKVQ*G cleavage sites between the VPgs at either the P_4, P_1 or P_1' position. These variants present a unique genetic system defining the cleavage signals recognized in 3C^{pro}-catalyzed proteolysis. We propose a recognition event in the *cis* cleavages of the polyprotein P2–P3 region, and we present a hypothesis why the poliovirus genome does not tolerate two tandemly arranged VPg sequences.

Keywords: aberrant processing/3C^{pro} cleavage site mutants/poliovirus/replication blocks/RNA recombination

Introduction

Genetic variation of RNA viruses results from high frequencies of misincorporation of nucleotides in the absence of error-correcting mechanisms, and recombination (King, 1988a; Holland *et al.*, 1992; Lai, 1992). The mechanism of homologous recombination occurring during the replication of poliovirus, a single-stranded RNA virus, has been investigated for decades. Generally, these studies involved two genetically distinct genomes, scoring for recombinants either by selection or by analysis of amplified genome sequences (reviewed in Wimmer *et al.*, 1993).

We have recently studied a genetic event in poliovirus replication that leads, inadvertently, to the deletion of a genome segment (Cao *et al.*, 1993). It occurs during the replication of quasi-infectious (*qi*) poliovirus RNAs into which two tandemly arranged, nearly identical coding sequences of VPg were engineered (Cao *et al.*, 1993; see Figure 1A). The term *qi* phenotype has been introduced to describe an RNA genome that can replicate in transfected cells at greatly reduced levels without producing detectable progeny virus. If viable viruses do arise from transfections with *qi* RNA, their genomes are altered to allow a full cycle of proliferation (Gmyl *et al.*, 1993; Cao and Wimmer, 1995). In the case of the *qi* poliovirus 2VPg-containing genome, progeny virus had always lost one complete VPg coding sequence. The deletion was precise in that the remaining VPg had the exact sequence as in the original 2VPg-containing *qi* genome (Cao *et al.*, 1993).

The strategy of constructing poliovirus genomes with 2VPgs was inspired by the observation that aphthovirus genomes encode three different VPgs in tandem (Forss *et al.*, 1984). Aphthoviruses (foot-and-mouth disease virus, FMDV) belong to the family Picornaviridae, as does poliovirus. These plus-stranded RNA viruses all contain genomes which are covalently linked to VPg at the 5′ end and polyadenylylated at the 3′ end (Figure 1A). All their translatable information is expressed in the form of a polyprotein that is cleaved by virus-encoded proteinases (Wimmer *et al.*, 1993). Experiments described here have allowed us to analyze the mechanism by which one of the VPg coding sequences in a 2VPg-containing genome is deleted. The results unambiguously show that homologous recombination contributes to the deletion, but 'homologous loop-out deletion' may also be involved in this event.

Homologous recombination requires extensive sequence homology between viral genomes at the site of cross-over (Wimmer *et al.*, 1993). We have eliminated this opportunity in a 2VPg-containing genome by designing two VPg coding sequences that differ by 36%. We had expected that such an alteration of the genotype would be lethal. However, to our surprise, such a 2VPg-containing genome, while still *qi*, generated progeny viruses that had eliminated the possibility of proficient 3C^{pro}-mediated proteolytic processing between the two VPgs. These experiments have produced a unique genetic test for the nature of a cleavage signal of 3C^{pro}-mediated proteolysis. They have also led to a new hypothesis of *cis* cleavages in the P2–P3 region of the polyprotein and to an explanation of why poliovirus, in contrast to aphthovirus, cannot tolerate two VPgs in tandem.

Results

Mechanism of VPg deletion in 2VPg-containing poliovirus RNAs

The deletion of one complete VPg coding sequence in progeny virus of pPVM-2VPg-2 RNA was originally studied using reverse transcription(RT)/polymerase chain reaction (PCR) techniques with primers C27 and C28 (Figure 1B). This did not allow us to determine whether the deletion event involves recombination between different RNA strands that had transfected the same cell independently, or between sibling RNA strands of a single

transfecting RNA. We therefore generated two genetically labeled genomes that were identical to pPVM-2VPg-2 except for four silent nucleotide substitutions flanking the 2VPg region (Figure 1B; pPVM-2VPg-3 and pPVM-2VPg-4).

In vitro translation of the pPVM-2VPg-2, -3 and -4 transcripts in HeLa cell-free extracts (Molla *et al.*, 1991) yielded patterns essentially identical to those reported previously (Cao *et al.*, 1993; Figure 2). Cleavage between the tandemly arranged VPgs occurred rapidly and aberrant processing was observed amongst the proteins of the 2BC-P3 region, with bands of P2-3AB, 2C-3AB and 3BCD emerging, whose identity was confirmed by immunoprecipitation (Figure 2, lanes 15–18). These translations confirmed that the open reading frame of the polyprotein was intact in all constructs.

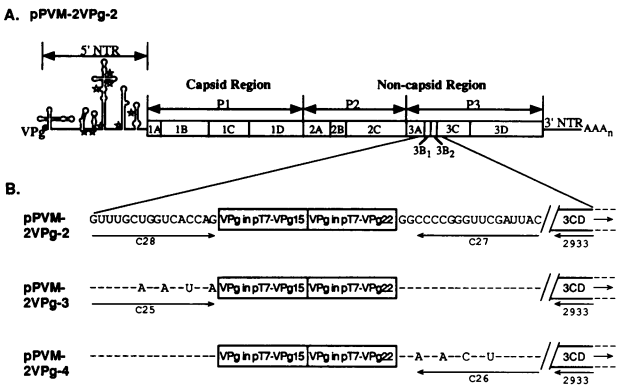

Fig. 1. Schematic depictions of the constructs containing 2VPg coding sequences in poliovirus genomes. (**A**) Structure of the construct pPVM-2VPg-2; the nucleotide sequences, which represent the VPgs in pT7-VPg15 and pT7-VPg22, were arranged in the genome between 3A and 3C (3B = VPg, Cao *et al.*, 1993). Viruses derived from pT7-VPg15 and pT7-VPg22 were previously characterized. They were indistinguishable from wild-type virus derived from pT7PV1–5 (Kuhn *et al.*, 1988). (**B**) The wild-type nucleotide sequences located at the 3′-end of 3A and the 5′-end of 3C which were used for RT/PCR analysis are shown for construct pPVM-2VPg-2. Nucleotide sequences of pPVM-2VPg-3 and -4 which are different from that of the construct pPVM-2VPg-2 are shown, and the dashed line represents identical nucleotides between pPVM-2VPg-2, -3 and-4. Primers used for RT/PCR are indicated below the drawing of each construct in (B). Arrows indicate the polarity of the primers.

Transfection of either pPVM-2VPg-3 or -4 RNA onto HeLa monolayers produced a cytopathic effect (CPE) indistinguishable from that of the pPVM-2VPg-2 RNA. As reported, the transfection efficiency for all RNAs was low (4–5 p.f.u./μg), but viruses recovered from transfected cells grew with *wt* phenotypes (data not shown). Sequence analyses confirmed that one complete VPg coding sequence was deleted, and the genetic marker at amino acid six (leucine) of the 5′-most VPg remained in the recovered viral genome. Therefore, the deletion of this one complete set of VPg amino acid sequence was equivalent to the deletion of the 3′-most VPg sequence. In order to determine whether this was the result of intergenomic recombination, pPVM-2VPg-3 and -4 RNAs were mixed in different ratios (pPVM-2VPg-3/pPVM-2VPg-4 = 1/4, 1/2, 1/1, 2/1, 4/1; Figure 3B). A total of 5 μg of each RNA mixture was co-transfected onto HeLa monolayers. Individual samples of pPVM-2VPg-3 and -4 RNAs were used as controls (Figure 3B). CPE had progressed to completion with all transfections within 3 days. Total cell lysates were harvested, frozen and thawed three times, and stored as virus stocks.

All viruses recovered from these experiments are predicted to retain only one VPg sequence. If homologous recombination had occurred between the two genetically distinct genomes pPVM-2VPg-3 and -4 (mechanism I), progeny virus would inherit either the extra two genetic markers or regain the wild-type genotype of pT7-PVM (Figure 3B; genotype 'b' or 'c', respectively). However, if all progeny viruses were generated only through homologous recombination between identical sibling strands of transfecting RNA (mechanism IIa) or intra-strand loop-out deletion (mechanism IIb), the viruses should only consist of the two genotypes 'a' and 'd' (Figure 3B). Regardless of the mechanism (I and II), the genotypes in

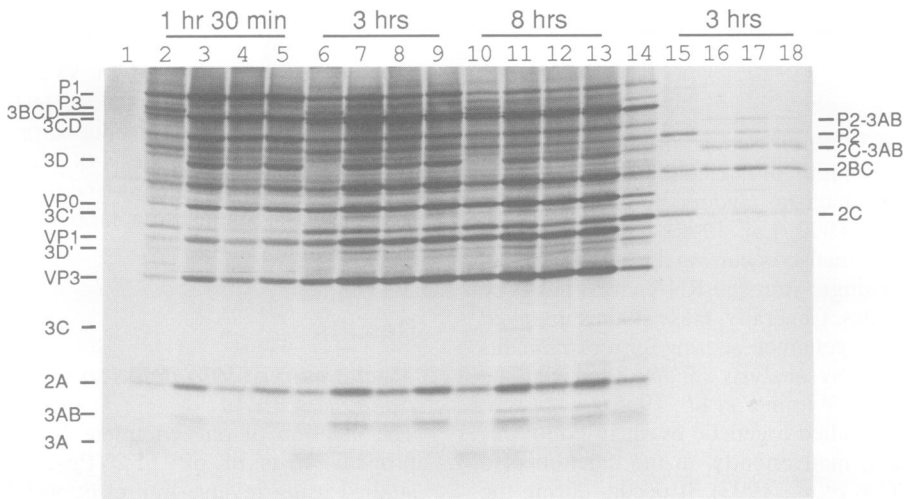

Fig. 2. *In vitro* kinetics of protein synthesis and processing directed by wild-type and 2VPg-containing RNAs. RNAs, transcribed *in vitro*, were translated in a HeLa cell extract from 1.5 to 8 h as indicated. The reaction mixtures were analyzed on a 10–20% gradient SDS–polyacrylamide gel. Lanes 2, 6, 10 and 15, reactions with pT7-PVM RNA; lanes 3, 7, 11 and 16, reactions with pPVM-2VPg-2 RNA; lanes 4, 8, 12 and 17, reactions with pPVM-2VPg-3 RNA; lanes 5, 9, 13 and 18, reactions with pPVM-2VPg-4 RNA; lane 1, no RNA; lane 14, [^{35}S]methionine-labeled proteins of PV1-infected HeLa extracts as marker. Lanes 15–18, polypeptides immunoprecipitated with anti-2C serum.

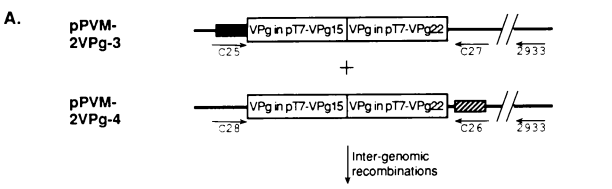

B.

Exp. No	pPVM-2VPg-3 / pPVM-2VPg-4	a (VPg)	b (VPg)	c (VPg)	d (VPg)
1	0/5	0	0	0	d
2	1/4	1	4	4	16
3	1/2	1	2	2	4
4	1/1	1	1	1	1
5	2/1	4	2	2	1
6	4/1	16	4	4	1
7	5/0	a	0	0	0

Fig. 3. Diagram of the theoretical prediction of intergenomic recombination results. (**A**) Schematic depiction of template RNAs pPVM-2VPg-3 and -4. Black and shaded boxes represent the genomic regions which contained heterologous nucleotides as genetic markers. Primers used in RT/PCR are shown below the drawing and the polarity of the primers is indicated by arrows. (**B**) Representation of intergenomic recombination between RNAs pPVM-2VPg-3 and -4. In all seven experiments of RNA co-transfections as indicated in (B), the total amount of RNAs was 5 μg. The recovered viruses which contained only one VPg but with different genetic markers are shown as in 'a', 'b', 'c' and 'd'; 'a', derived from template RNA pPVM-2VPg-3; 'd', derived from template RNA pPVM-2VPg-4; 'b' and 'c', derived from template switching between RNAs pPVM-2VPg-3 and -4, either inherited both genetic markers or no marker. Numbers shown in columns 'a', 'b', 'c' and 'd' indicated the predicted relative ratios of each recovered viral genome.

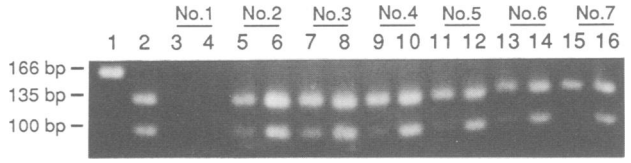

Fig. 4. RT/PCR analysis of products of intergenomic recombination between RNAs of pPVM-2VPg-3 and -4. Cytoplasmic RNAs were isolated at 6 h post-infection and the plus-strand RNAs were reverse transcribed and PCR amplified. PCR products were analyzed by agarose gel electrophoresis. Viruses used for infections in experiments 1–7 were derived from RNA co-transfections with RNA ratio 2VPg-3/2VPg-4 = 0/5, 1/4, 1/2, 1/1, 2/1, 4/1, 5/0. Lane 1, plasmid DNA of pPVM-2VPg-3 as template, and oligonucleotides C25 and C27 as primers. The product with 166 bp represented the 2VPg-containing genome; lane 2, plasmid DNA of pPVM-VPg-3 (a derivative of pPVM-2VPg-3 which contained only one VPg coding sequence as in pT7-VPg15) as template, oligonucleotides 2933, C27 and C25 as primers. In experiments 1–7, all cDNAs were generated from oligonucleotide 2933. The fragment with 135 bp indicated the specific PCR product derived from the one VPg genome 'a' and 'b' (see Figure 3) with primer 2933 and C25, whereas the fragment with 100 bp indicated the specific PCR products either derived from the one VPg genome 'b' (lanes 3, 5, 7, 9, 11, 13 and 15) with primer C25 and C26, or from the one VPg genome 'a' (lanes 2, 4, 6, 8, 10, 12, 14 and 16) with primer C25 and C27. As illustrated in Figure 3, viral genome 'a' and 'b' contained only one VPg, 'a' inherited the genomic marker as in pPVM-2VPg-3, 'b' inherited both genomic markers as in pPVM-2VPg-3 and -4.

experiments 1 and 7 (Figure 3B) should only be type 'd' or 'a', respectively.

If only mechanism I were operating, progeny viruses would be predicted to occur in the ratios given in Figure 3B, depending on the input RNA concentrations (experiments 1–7). To test this prediction, RNAs from the mixture of progeny viruses, harvested after co-transfections in different concentrations, were purified and subjected to RT/PCR. In order to minimize the bias of RT/PCR due to different primers, oligonucleotide 2933 was selected for the reverse transcription reaction for templates 'a', 'b', 'c' and 'd' (Figure 3A). cDNAs, derived from the progeny virus RNAs and primer 2933, were divided into four equal amounts and amplified by four PCRs, using primer pairs C25 and C27, C25 and C26, C28 and C27, C28 and C26, while primer 2933 was not removed from the mixtures. Together, these primers had the propensity to generate two bands: 100 bp for all primer combinations mentioned above, and 135 bp for the reaction with primers C25 or C28 and 2933. This 135 bp reaction product served as an internal control for the PCR.

Figure 4 shows the results of PCRs performed with primer pairs C25 and C26 (lanes 3, 5, 7, 9, 11, 13 and 15) or with C25 and C27 (lanes 4, 6, 8, 10, 12, 14 and 16). In experiment 1 (lanes 3 and 4), progeny virus was derived only from pPVM-2VPg-4 RNA transfection; hence, no PCR products were detectable due to the mismatch between primer C25 and the cDNA template derived from viral RNA 'd'. In experiment 7 (lanes 15 and 16), where the progeny virus originated from pPVM-2VPg-3 RNA transfection, a large PCR fragment of 135 bp appeared in both reactions which derived from primer pair C25 and 2933 (lanes 15 and 16), but the 100 bp band that represented viral genome 'a' was detectable only with primer pair C25 and C27 (lane 16) and not with C25 and C26 (lane 15). These two control experiments indicated that the four varying nucleotides at the 3′-end of each primer conferred to the PCR the necessary specificity.

In experiments 2–6, where progeny viruses derived from co-transfections of RNAs pPVM-2VPg-3 and -4 with molecular ratios of 1/4, 1/2, 1/1, 2/1 and 4/1, the 100 bp fragment (primer pair 25 and 27) originating from genotype 'a' was generated at nearly the same level as the 135 bp control fragment (Figure 4, lanes 6, 8, 10, 12 and 14). In contrast, primer pair C25 and C26 would generate the 100 bp fragment only from recombinant genome 'b', as seen in lanes 5, 7, 9, 11 and 13. It was generated at very low levels compared with the control fragment (135 bp). These results, although not quantitative, are at variance with the predicted ratios of the appearance of genotypes 'a' and 'b' (Figure 3B). For example, in experiment 4 genome 'b' was detected at a level of ~10% of genome 'a' (Figure 4, lanes 9 and 10) and not at the same level as predicted. Similar RT/PCR results were obtained with primer pair C28 and C26, and primer pair C28 and C27, in analyses of genomes 'c' and 'd' (data not shown).

To confirm the ratio of genotypes in experiment 4, a large number of progeny viruses were plaque purified, which originated from a transfection experiment with equal amounts of RNA. RNAs from individual isolates were then directly sequenced using oligonucleotide 2933 as primer. The results from 30 isolates revealed 14 genomes of type 'a', 13 genomes of type 'd', two genomes of type 'b' and one genome of type 'c' (Table I). Thus, recombinants arising from cross-over between pPVM-2VPg-3 and -4 RNAs (mechanism I) accounted for ~10% of the total progeny viruses.

Genetic events with viral RNA encoding two heterologous VPg sequences

The data presented so far shed light on the mechanism by which the VPg sequence is deleted. They do not explain why poliovirus, in contrast to aphthovirus (Falk *et al.*, 1992), cannot tolerate two VPg sequences. We therefore thought to develop a strategy for preventing the deletion event, hoping that the genetic response of the virus would reveal the block leading to the *qi* phenotype in the 2VPg-containing RNAs. A viral genome was constructed (Figure 5A) in which the coding sequence for the 3′-most VPg was altered, mostly in the wobble position, without changing the amino acid sequence (Figure 5B). The extent (36%) and nature of the sequence differences between the two VPg sequences made it unlikely that homologous recombination could occur (Kirkegaard and Baltimore, 1986; Romanova *et al.*, 1986; Wimmer *et al.*, 1993). Translation of pPVM-2VPg-5 transcript in a HeLa cell-free extract generated the same processing patterns as resulted from the other 2VPg-containing RNAs (data not shown).

pPVM-2VPg-5 RNA was transfected onto HeLa cell monolayers. CPE developed at 72 h post-transfection, 50 h later than with the pPVM-2VPg-2, -3 or -4 RNAs. This delay of CPE was reproducible over more than 20 independent transfections. Genomic RNAs of 26 viruses that were directly plaque purified from the transfections were sequenced through the region encoding the 2VPg sequences. The results were most surprising. The genomes of all 26 variants had retained both VPg sequences, but the $3C^{pro}$-specific cleavage signal (**AKVQ*G**) between the VPgs was mutated such that cleavage was unlikely or slow. The 26 sequences could be divided into eight groups of revertants (Figure 6, rV1–rV8). Most of the variants had amino acid substitutions in the P_4 position (**A**KVQ*G): five contained threonine (rV1), one contained serine (rV2) and three contained glutamic acid (rV3) instead of alanine at P_4 (Figure 6). A three-base deletion in rV4 RNA also had the effect of modifying the P_4 position to an unfavorable residue (threonine) (Figure 6). Fourteen variants had changes in the P_1 position of the scissile bond (AKV**Q***G): 13 carried histidine (rV5) and one glutamic acid (rV6) at this position. Finally, two variants (rV7 and rV8) had changes (aspartic acid and arginine, respectively) in P_1' of the scissile bond (AKVQ*G**G**).

The search for viable variants was extended as follows. Several transfections with pPVM-2VPg-5 RNA were allowed to proceed to complete CPE. Total RNA was isolated from each cell lysate and analyzed by RT/PCR using primers 2910 and 2912. The results showed a single prominent band, and several weaker bands, all of which migrated in the size range of a 2VPg-containing genome (data not shown). This suggested deletion events spanning different segments of the VPg sequences. Viruses from these transfections were plaque purified and their RNAs subjected to sequencing. Seven new viable variants emerged (Figure 6, rV9–rV15). In contrast to the first set of variants (isolated by direct plaque isolation of transfections), most of these new variants (originating from pools of variants in total lysates) carried amino acid deletions in the 2VPgs region. Apparently, these deletion variants expressed growth advantages over the other variants in tissue culture. The deletions were random and, in some cases, were accompanied by additional amino

Table I. Results of genomic analysis from co-transfections of RNAs pPVM-2VPg-3 and pPVM-2VPg-4

RNA ratio of 2VPg-3/2VPg-4	Numbers of viral genome				Genome ratio
	a	b	c	d	a + d/b + c
1/1	14	2	1	13	27/3

Genome structures of a, b, c and d are illustrated in Figure 3B.

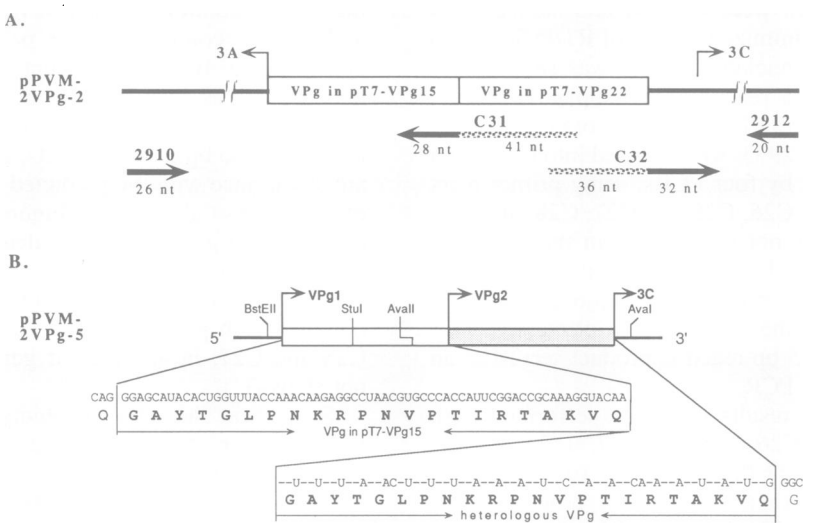

Fig. 5. Schematic depiction of the double VPg construction of pPVM-2VPg-5. (**A**) The plasmid pPVM-2VPg-2 was used as template for generating a PCR fragment for the construction of pPVM-2VPg-5; the position and the polarity of the PCR primers are indicated. Black bars represent nucleotide sequences which are complementary to the template and hatched bars represent nucleotides of which only 64–66% are complementary to the template. Numbers representing the length of the primers are indicated below the drawing of the primers. (**B**) The open box represents the VPg sequences in the VPg mutagenesis cartridge pT7-VPg15 and the stippled box represents the VPg sequences which share only 64% homology with that of pT7-VPg15. The nucleotide sequences, which are different from that in pT7-VPg 15, are shown, while the identical nucleotides are indicated by dashes.

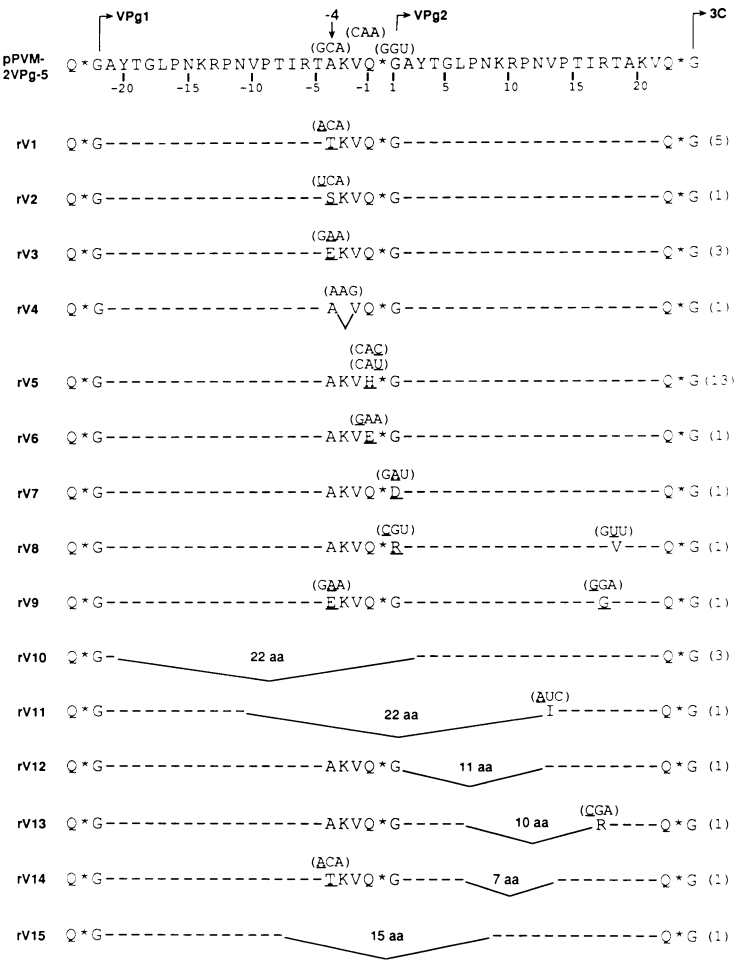

Fig. 6. Schematic representation of modified viral genomes derived from transfection of RNA pPVM-2VPg-5. The amino acids in the VPg region of pPVM-2VPg-5 are shown. Nucleotide sequences which encode the amino acids Ala, Gln and Gly at position –4, –1 and 1, respectively, are shown in parentheses above the corresponding amino acid sequences. Numbers which represent the positions of the amino acids in the VPg region are indicated below the drawing of pPVM-2VPg-5. Number 1 started from the first amino acid in the 3C-related VPg. The amino acids in the variants, which are identical to that of pPVM-2VPg-5, are aligned in a dashed line, except for the region including the active cleavage sites of $3C^{pro}$. Nucleotides and amino acids which are different from the corresponding sequences in pPVM-2VPg-5 are underlined. The solid lines represent amino acid deletions in the variants. The numbers in parentheses represent the frequency for each of the variants.

acid substitutions. Two variants had one entire VPg sequence removed (rV10 and rV11). The significance of these variations, apparently generated in this experiment to prevent aberrant cleavages in the P2–P3 region of the polyprotein, will be discussed later.

Growth and processing phenotypes of the pPVM-2VPg-5 variants

Analyses of the growth properties of the variants at different temperatures revealed generally medium to small plaque sizes, with no clear *ts* phenotypes (Table II). Variants rV10 and rV11 grew with *wt* properties, as expected. *In vivo* labeling of viral proteins of the variants 5 h after infection on HeLa cells showed that, in all cases, processing between the 2C*3A cleavage site was no longer inhibited (Cao *et al.*, 1993). However, the mobilities of the 3AB proteins were altered (data not shown; see also Figure 7). This was further analyzed for variants rV3, rV6, rV12, rV14 and rV15 by pulse–chase experiments (5 min pulse with [^{35}S]methionine, followed by chase periods of 0, 5, 10, 20 and 60 min). PAGE analyses on 10–25% gradient gel are shown in Figure 7. Except for the region of the 3AB-related proteins, all variant processing patterns were similar to that of *wt* virus. Variant rV6 with a cleavage site mutation in P_1 showed a band corresponding to $3AB_1B_2$ that was readily processed to $3AB_1$ (lanes 6–10). This observation indicated that the glutamic acid residue in P_1 interfered only weakly with cleavage. On the other hand, cleavage of $3AB_1B_2$ to $3AB_1$ was nearly abolished in rV3 encoded proteins (lanes 11–15). Therefore, the glutamic acid residue in the P_4 position has a more severe effect that interfered with the $3C^{pro}$ cleavage activity. A similar effect of the *P4* mutation was also observed for proteins encoded by variant rV14 (lanes 21–25). Although the cleavage site between $3B_1$ and $\Delta 3B_2$ in rV12 was unchanged, a band designated $3A\Delta(B_1B_2)$ appeared during the pulse that was rapidly processed to $3AB_1$ (lanes 16–20). Finally, in rV15 where the entire cleavage signal plus surrounding amino acids had been deleted, a band with the mobility of 3AB never appeared, as expected, but band $3A\Delta(B_1B_2)$ was observed (lanes 26–30). It should be pointed out that the pulse–chase experiments have been performed with both the first and the seventh passaged viruses of revertants rV3, 6, 12, 14

Table II. Phenotypic analysis of the revertant viruses derived from pPVM-2VPg-5 RNA transfection

	32°C		37°C		39°C	
	Size[a]	Titer[b]	Size	Titer	Size	Titer
PVM	60	5×10^7	100	2×10^9	90	6×10^8
rV1	30	5×10^7	60	1×10^9	40	5×10^8
rV2	30	5×10^7	40	4.5×10^8	10	1×10^8
rV3	10	5×10^7	80	3×10^8	60	8×10^7
rV4	10	1×10^7	50	3×10^8	20	5×10^7
rV5	10	2×10^7	50	4×10^8	40	5×10^7
rV6	10	5×10^7	80	1×10^9	40	5×10^8
rV7	60	5×10^7	70	8×10^8	40	6×10^8
rV8	60	1×10^8	70	5×10^8	50	1×10^8
rV9	10	4×10^7	80	7×10^8	60	1×10^8
rV10	60	5×10^7	100	1.5×10^9	90	1×10^9
rV11	60	5×10^7	80	1×10^9	70	5×10^8
rV12	60	7.5×10^7	70	8.5×10^8	90	5×10^8
rV13	50	1×10^7	60	1.5×10^8	20	6.5×10^7
rV14	60	5×10^7	80	6.5×10^8	80	1×10^9
rV15	30	1.5×10^7	60	2×10^8	30	3×10^8

[a]The size of the wild-type virus PVM was defined as 100, all others were compared with wild-type.
[b]Unit of the virus titers: p.f.u./ml.

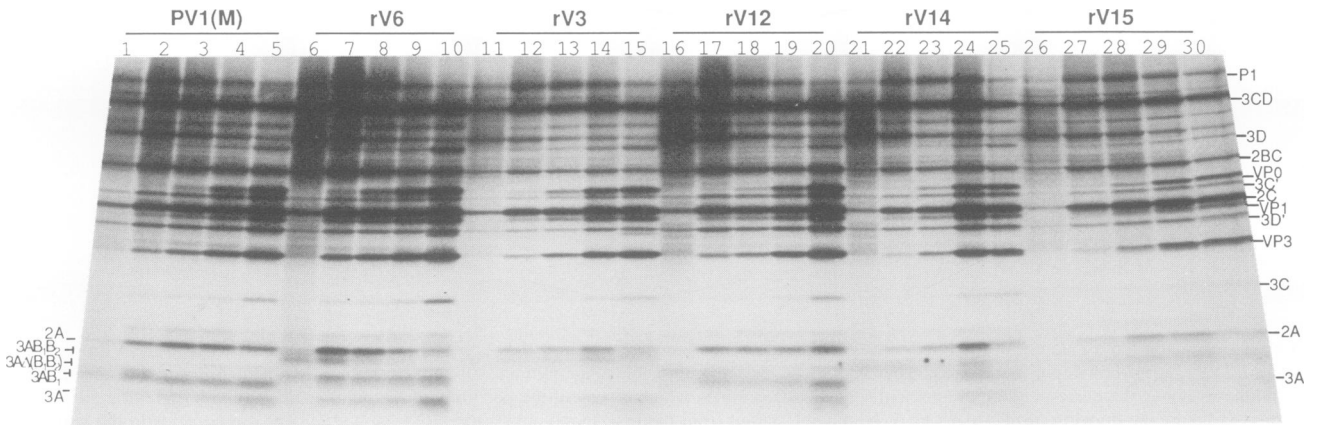

Fig. 7. *In vivo* kinetics of protein synthesis and processing directed by wild-type or revertant viruses. Viruses are pulse labeled with [^{35}S]methionine for 5 min and followed by different chase periods. Viral proteins were analyzed on a 10–25% SDS gradient gel. Lanes 1, 6, 11, 16, 21 and 26, 0 chase time; lanes 2, 7, 12, 17, 22 and 27, 5 min chase; lanes 3, 8, 13, 18, 23 and 28, 10 min chase; lanes 4, 9, 14, 19, 24 and 29, 20 min chase; lanes 5, 10, 15, 20, 25 and 30, 60 min chase.

and 15. The protein processing patterns of the two passaged viruses were identical (data not shown). Only the result of the seventh passaged viruses are shown in Figure 7.

Confirmation of the phenotypes of pPVM-2VPg-5 variants

In order to confirm that the observed phenotypes in variants were not the result of additional mutations in protein coding sequences outside the 3AB region, the 3AB coding sequences of variants rV3, rV6, rV10 and rV15 were reconstructed into the infectious cDNA clone pT7-PVM (Cao *et al.*, 1993). These variants were chosen because they represent the different variant groups. To achieve this, purified viral RNAs were reverse transcribed using oligonucleotide 2912 as primer, and the cDNAs were PCR amplified with primers 2912 and 2910 (see Figure 5A). DNAs, containing VPg sequences, were isolated by *Hpa*I and *Bgl*II restriction enzyme digestion, and inserted into the corresponding sites of pT7-PVM. The sequences in the 3AB region of the resulting cDNA plasmids (pPVM-rV3, -rV6, -rV10 and -rV15) were verified with those corresponding to the variant viruses. Transcript RNAs of these constructs were then transfected onto HeLa cell monolayers. All transfections produced complete CPE at much earlier times than that with pPVM-2VPg-5 RNA: with pPVM-rV3 at 36 h, with pPVM-rV6 at 48 h, with pPVM-rV10 at 20 h and with pPVM-rV15 at 44 h. Viruses isolated from the transfection yielded phenotypes resembling those of the original variant viruses as in Table II (data not shown). This indicated that the mutation mapping to the VPg-encoding region derived from the replication of the *qi* pPVM-2VPg-5 genome was responsible for the observed phenotypes.

Does 3AB exist in infected cells in modified forms?

PAGE analyses repeatedly revealed two bands closely migrating in the region of polypeptide 3AB. As can be seen in Figure 7, the upper band of 3AB disappeared during the conditions of the chase (compare lane 2 with lane 3). We have analyzed this phenomenon by making use of the two VPg-specific antibodies C7 (raised against

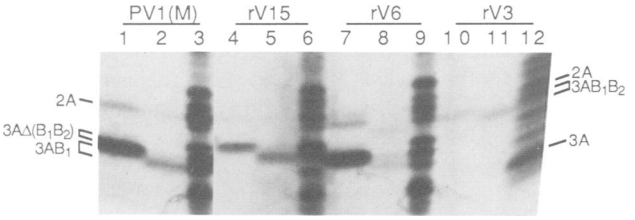

Fig. 8. Immunoprecipitation of *in vivo* labeled viral proteins from wild-type and variant virus infections. Viruses are infected onto HeLa cells with MOI 30 and the viral proteins, labeled with [^{35}S]methionine at 5 h post-infection for 15 min, were immunoprecipitated with anti-VPg serum C7 (lanes 1, 4, 7 and 10) and N10 (lanes 2, 5, 8 and 11). Total cytoplasmic extracts of [^{35}S]methionine-labeled virus-infected HeLa cells are shown as controls (lanes 3, 6, 9 and 12). A 10–25% SDS gradient gel electrophoresis was used.

seven C-terminal residues of VPg) and N10 (raised against 10 N-terminal residues of VPg). Antibody C7 was found to recognize only the upper band in cell lysates infected with PV1(M). This was also true for lysates infected with viruses rV15, rV6 and rV3 (Figure 8, lanes 1, 4, 7, 10), except that the immunoprecipitated band had mobilities according to the variation in size (note that in lane 10 only a band corresponding to an unprocessed $3AB_1B_2$ was immunoprecipitated; see also Figure 7). In contrast, antibody N10 recognized only the lower bands (that appeared during the chase) which migrated slightly faster (Figure 8, lanes 2, 5, 8, 11). An exception is lane 8, where $3AB_1$ separated into two bands. Currently, we have no explanation for this phenomenon.

Discussion

Genetic recombination in poliovirus replication occurs by a copy-choice mechanism during minus-strand synthesis (King, 1988a; Kirkegaard and Baltimore, 1986; Romanova *et al.*, 1986; Wimmer *et al.*, 1993). Regardless of whether the recombinants have been scored by selection (Wimmer *et al.*, 1993) or by analysis of progeny strands without selection (Jarvis and Kirkegaard, 1992), all studies reported so far have been confined to cross-overs between viral RNAs of different genotypes originating from distinct viral strains used in co-infections. The deletion occurring in *qi* viral genomes containing nearly identical nucleotide sequences of 2VPgs is different (pPVM-2VPg-1 and -2; Cao *et al.*, 1993). Here, a block in replication can be removed without genetic interactions between genetically different genomes. The mechanism of this deletion seems to obey the rules of homologous recombination in poliovirus replication (Kirkegaard and Baltimore, 1986; Romanova *et al.*, 1986): a strict polarity of the deletion that indicated cross-over during minus-strand synthesis, and an absolute precision of the deletion (Cao *et al.*, 1993). The question remained, however, whether the deletion occurred by recombination between RNA strands originating from different infecting genomes (mechanism I), by recombination between sibling strands within a replication complex (mechanism IIa) or by an intra-strand loop-out mechanism in which the minus strand would 'skip' a sequence segment and reanneal precisely 66 nucleotides upstream on the template (mechanism IIb).

The data presented here clearly show that both mechanisms I and II lead to the observed deletion, but the experimental design does not allow us to differentiate between IIa and IIb. Although known to occur readily in many RNA replicating systems, we were surprised to observe mechanism I in the deletion of the VPg sequence of the 2VPg-containing genomes. First, poliovirus RNA replication is thought to occur in tight membrane-bound replication complexes (Bienz *et al.*, 1980, 1987; Kuhn and Wimmer, 1987) that would seem to greatly favor genetic exchanges between sibling strands and, second, the relief from the replication block does not require interaction between RNA strands of two genetically different genomes. It can be concluded that recombination between sibling strands is common in poliovirus genome replication, and it is likely to occur frequently in all RNA replication systems for which homologous recombination has been demonstrated. This offers a highly selective advantage for these RNA viruses as it can lead to the elimination of spontaneous lethal mutations, and it may aid in the adaptation to a new environment.

Cross-overs within the nearly identical VPg sequences of pPVM-2VPg-1, -2, -3 and -4 RNAs always occurred downstream of amino acid six (leucine) of the 5′-most VPg. This polarity is essentially equivalent to the removal of the 3′-most VPg. Analysis of the nucleotide sequences of both tandemly arranged VPgs revealed that seven AA nucleotide pairs are present downstream of amino acid six of both VPgs, but none upstream of this residue. King (1988b) has suggested that template switches in homologous recombination of poliovirus RNA may be preferably occurring at such AA pairs. Our data support this hypothesis.

What is the nature of the replication block in the 2VPg-containing pPVM-2VPg-2 RNA that leads to the complete selection of a *wt* RNA strand which contains only one VPg sequence? *In vitro* translation of RNAs containing two tandemly arranged VPg sequences has indicated aberrant proteolytic processing events of the polyprotein (Cao *et al.*, 1993; and data obtained in this study). However, the disturbance in the cleavage pathway in the *in vitro* assay is not complete, and all essential viral proteins were produced after prolonged incubation. Perhaps *in vivo* the processing block exerts its influence in a very early event of genome replication which is not readily detected by *in vitro* translation.

In an attempt to find an answer to this question, we changed the nucleotide sequence of the 3′-most VPg, thereby eliminating the 2VPg-containing genome's clever device to delete one of the VPg sequences by homologous recombination. The genetic response of poliovirus to this challenge came as a complete surprise.

The transcripts of pPVM-2VPg-5 were also *qi*, just like pPVM-2VPg-2 transcripts, but the appearance of viable variants was much delayed as compared with the latter. Two classes of viable variants of pPVM-2VPg-5 were observed: class I with point mutations leading to amino acid exchanges in positions P_4, P_1 and $P_{1'}$ (**AKVQ*G**) of the $3C^{pro}$-specific cleavage signal between the two VPg peptides, and class II with deletions in the 2VPg-encoding region, sometimes with an additional amino acid substitution (Figure 6). Both classes of mutations inhibit or eliminate the cleavage $3AB_1{*}B_2CD$ to $3AB_1 + 3B_2CD$ in the P3 region of the polyprotein (Figure 9B and C).

Why does the virus strive to avoid the generation of

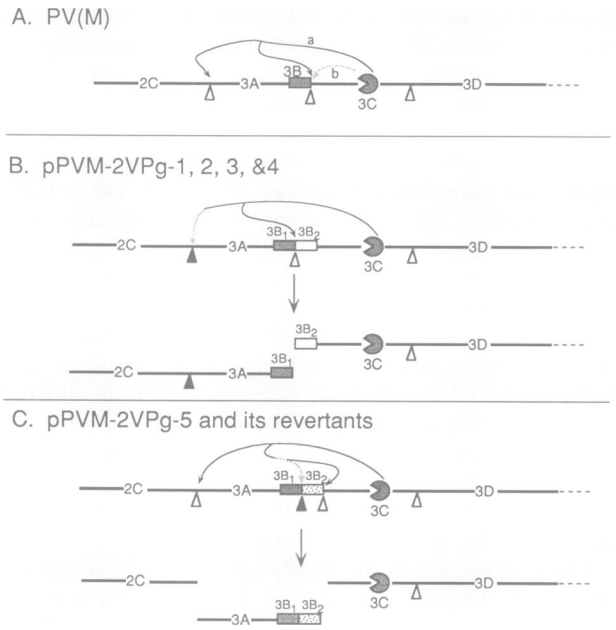

Fig. 9. Potential mechanisms for *cis* cleavage of the 2C-3A site. Cleavage of the wild-type polypeptide 2C-P3 is shown in (**A**); cleavage of the 2VPg-containing polypeptide 2C-3A(B_1B_2)3CD is shown in (**B**); cleavage of the revertant polypeptide 2C-3A(B_1B_2)3CD is shown in (**C**). Open triangles and solid arrows indicate the favorable cleavage sites and passways; shaded triangles and dashed arrows indicated the unfavorable cleavage site and passways. The darker shaded box represents the VPg in pT7-VPg-15. The open box represents the VPg in pT7-VPg22. The lighter shaded box represents the heterologous VPg.

$3B_2$CD? It is known that the naturally occurring cleavage product $3CD^{pro}$ has multiple functions in poliovirus replication. (i) $3CD^{pro}$ is a proteinase required for capsid precursor P1 processing that may possibly carry out all other Q*G cleavages as well (Lawson and Semler, 1991), and $3CD^{pro}$ cleaves membrane-associated 3AB to 3A and VPg (Lama *et al.*, 1994). (ii) $3CD^{pro}$ forms a complex with 3AB that, in turn, binds to the 5′-terminal cloverleaf of the viral genome (Harris *et al.*, 1994). Formation of this RNP is essential for poliovirus genome replication (Xiang *et al.*, 1995). (iii) Complex formation between 3AB and $3CD^{pro}$ leads to accelerated autoprocessing of $3CD^{pro}$ under formation of RNA polymerase $3D^{pol}$ (Molla *et al.*, 1994). It is conceivable that the linkage of $3B_2$, a highly active peptide of 22 amino acids, to the N-terminus of $3CD^{pro}$ interferes with one or all of the functions described above.

In *wt* poliovirus, the P3 region of the polyprotein is very rapidly cleaved to 3AB + $3CD^{pro}$, simultaneously with, or soon after, the separation of P2 and P3 peptides. Both cleavage events occur most likely in *cis* (Figure 9A, mechanism a). The P3 region of pPVM-2VPg-2 ($3AB_1B_2CD$) can theoretically undergo autocleavage to either $3AB_1$ + $3B_2$CD (pathway I) or $3AB_1B_2$ + $3CD^{pro}$ (pathway II). The nature of the mutations in the variants of pPVM-2VPg-5 implies that pathway I in the 2VPg-containing polypeptides is the preferred pathway (Figure 9B). This, in turn, suggests that the selection of the cleavage site in *wt* polyprotein $3AB_1$*CD, or in mutant polyprotein $3AB_1$*B_2*CD, involves recognition of protein structures upstream of the 3B sequence. This may include the regions of 2C and 3A (Figure 9A, recognition mechanism a). A direct 'upstream search' of the $3C^{pro}$ active site in $3CD^{pro}$ for the closest Q*G cleavage signal can therefore be excluded (Figure 9A, recognition mechanism b). Based on these considerations, it becomes apparent that a polyprotein of the structure $3AB_1$*B_2*CD is cleaved to $3AB_1$ + $3B_2$CD. The cleavage site variants of pPVM-2VPg-5, however, avoid pathway I by mutations of the cleavage site between $3B_1$*$3B_2$ and, instead, enter cleavage pathway II (Figure 9C). The resulting polypeptide $3AB_1B_2$ is apparently permissive and can subsequently be processed, however slowly, to $3AB_1$ and B_2 in spite of the cleavage site mutations.

We are compelled to conclude that the rapid *cis* cleavages in the poliovirus polyprotein involve very complex and distant interactions of polypeptide chains. This also serves to explain why an interruption of the polyprotein by insertion of an IRES element at cleavage sites 2C*3A or 3AB*3CD is lethal (A.V.Paul and E.Wimmer, unpublished data).

Mutants rV10, rV11 and rV15 bypass the aberrant processing pathway by having deleted extended sequences in the $3B_1B_2$ region of pPVM-2VPg-5. Variant rV10 is of special interest because it lost a complete set of VPg coding sequence. In contrast to deletions with homologous VPgs in pPVM-2VPg-2, the deleted VPg is 5′-most. This clearly implies an unknown mechanism of deletion distinct from homologous recombination. Surprisingly, variant rV15 can proliferate with a VPg that is longer than *wt* VPg by seven residues; this aberration of the genome-linked protein may be the reason for the observed replication phenotype (Table II). Variants rV12, 13 and 14 have basic residues removed in $3B_2$ that appear to allow the cleavage products to function.

Of special interest are the cleavage site mutations of variants rV1–9 and rV14, that all map to the cleavage signal **AKVQ*G** between the two VPg peptides. Indeed, the viral response to construct pPVM-2VPg-5 represents a unique genetic system in which mutations mapping to the **AKVQ*G** cleavage site are observed that have been selected to avoid processing. This, in turn, reveals the relative importance of residues of the entire cleavage signal *in vivo*. The Q*G scissile bond is the hallmark of cleavage sites for $3C^{pro}$-like viral proteinases in numerous polyproteins of plus-strand RNA viruses (Semler *et al.*, 1981; Ypma-Wong *et al.*, 1988a,b). However, many cleavage sites in polyproteins of RNA viruses have been observed to carry a glutamic acid residue at P_1. This amino acid has never been found in P_1 sites of poliovirus polyproteins (Nicklin *et al.*, 1986; Kraeusslich and Wimmer, 1988). The fact that variant rV5 contains glutamic acid at the P_1 position shows that the poliovirus $3C^{pro}$ is greatly impaired in cleaving an E*G site.

The P_4 position of $3C^{pro}$-related cleavage sites of poliovirus polyproteins has long been recognized as an important determinant of cleavage efficiency. This involved sequence comparisons (Nicklin *et al.*, 1986), genetic manipulations of cleavage signals (Blair and Semler, 1991; Harris *et al.*, 1992) and cleavage kinetics of synthetic peptides using purified $3C^{pro}$ (Pallai *et al.*, 1989). The most favorable amino acid in P_4 is alanine, but other small aliphatic residues (e.g. valine) can also be accommodated. It is surprising, however, that replacement

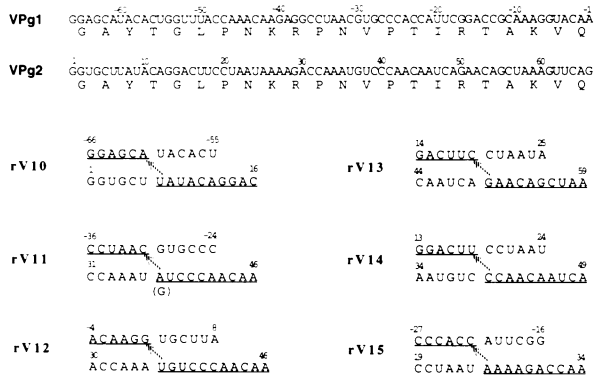

Fig. 10. Predicted cross-over sites of revertants rV10–rV15. VPg1 and VPg2 represent the 5′- and the 3′-most VPg in the genome of pPVM-2VPg-5, respectively. The first nucleotide of VPg2 starts as position number 1. Nucleotide sequences are written from the 5′ to 3′ end. Nucleotide sequences around the cross-overs in the revertants rV10–rV15 are underlined. Arrows indicate the predicted cross-over sites. Nucleotide in parentheses (see rV11) represents the original sequence in Vpg2.

of alanine in P_4 by a small serine (variant rV2) had a significant inhibitory effect on cleavage. The crystal structure of $3C^{pro}$ of human rhinovirus 14 (HRV14), a picornavirus closely related to poliovirus, has recently been solved (Matthews *et al.*, 1994). It was found that the S_4 pocket of this proteinase is small and hydrophobic, and that it best accommodates small and hydrophobic amino acids in P_4 of the substrate (e.g. VVVQ*G; Matthews *et al.*, 1994). By comparison of the closely related enzymes of HPV14 and poliovirus, the S_4 pocket of poliovirus $3C^{pro}$ is also small and hydrophobic. When the substrate enters the binding pocket, a serine in P_4 requires desolvation of its polar side chain with no opportunity for recovering this energy by hydrogen bonding in S_4. This explains why the replacement of alanine in P_4 by threonine, serine or glutamic acid in rV1, rV2 or rV3, respectively, inhibits the cleavage between $3AB_1$*B_2CD. It also sheds light on the virus' strategy of generating processing intermediates with a desired long half-life, such as $3CD^{pro}$. This protein carries an unfavorable threonine in P_4 of its 3C*D cleavage site (Pallai *et al.*, 1989; Harris *et al.*, 1992).

Analysis of the cross-over regions of the viable variants rV10–rV15 of pPVM-2VPg-5 RNA is shown in Figure 10. We have not been able to detect secondary RNA structures in these areas that would favor deletions by loop-out mechanisms. Our data suggest that the cross-over sites are not entirely random. In the case of rV11 and rV12, both share the same template switching site. From the nucleotide sequences around the cross-over regions in these revertants, however, we have not been able to decipher a pattern in what appears to be non-homologous recombination.

If duplication of VPg sequences in the poliovirus genome is deleterious for replication, why does FMDV retain three tandemly arranged VPg sequences? First, inspection of the coding sequences reveals that they are heterologous (35–44%), eliminating the possibility of deletion by recombination. Second, it is likely that the cleavage intermediates in the P3 region of the FMDV polyprotein have evolved to perform functions that differ from that of the poliovirus counterpart. For example, the capsid P1 precursor of FMDV is cleaved by $3C^{pro}$ and not by $3CD^{pro}$ and, indeed, special functions for FMDV $3CD^{pro}$ have not been described. Perhaps cleavage intermediates such as 3ABB and 3BCD are favorable in FMDV replication (Falk *et al.*, 1992).

Materials and methods

Cells and viruses

HeLa cells (R19) were grown in Petri dishes in Dulbecco's modified Eagle's (DME) medium supplemented with 5% fetal bovine serum, 100 U/ml penicillin and 100 mg/ml streptomycin sulfate (Gibco-BRL). Polioviruses were derived from single plaque isolates resulting from infectious RNAs transcribed *in vitro* (van der Werf *et al.*, 1986).

Construction of recombinant plasmids

Plasmid pPVM-2VPg-2 contained two nearly identical, tandemly arranged coding sequences of the genome-linked protein, VPg. Specifically, in position 6, the VPg sequence in VPg15 (the 5′-most VPg) contained a leucine (UUA, wild-type sequence), whereas in VPg22 (the 3′-most VPg) it was a methionine (AUG). The viability of this plasmid RNA in HeLa cells was characterized previously (Cao *et al.*, 1993).

Construction of plasmids pPVM-2VPg-3 and pPVM-2VPg-4. In order to create the genetic markers located outside the VPg region of the 2VPg-containing plasmids, combination PCRs were performed. In the first step of PCR, DNA plasmid pPVM-2VPg-2 was used as template. Oligonucleotides 2910 (GGGTTGGATAGTT-AACATCACCAGCC, plus strand, nucleotide positions 5230–5255) and C23 (CCTTGATG-TCCTG-CAAACAGTTTATACATGAC, complementary to nucleotide positions 5342–5373), as well as C24 (GCAGGACATCAAGGAGCATA-CACTGGTTTACC, plus strand, nucleotide positions 5360–5391) and 2912 (CCTGCTTGATCTTCGAGCGC, complementary to nucleotide positions 5618–5637) were used as external primers for generating the two primary PCR fragments 1 (144 bp) and 2 (344 bp), respectively, for the construction of DNA plasmid pPVM-2VPg-3. Oligonucleotides 2910 and C21 (AAAGCCTGGTCCTTGTACCTTTGCGG, complementary to positions 5424–5449), as well as C22 (GGACCAGGCTTTGATTACGC-AGTGGC, plus strand, positions 5438–5463) and 2912 were used as external primers for generating the two primary PCR fragments 3 (286 bp) and 4 (200 bp), respectively, for the construction of DNA plasmid pPVM-2VPg-4. Oligonucleotides C23 and C24 were complementary to each other and contained four nucleotide substitutions (underlined) corresponding to the C-terminus of the 3A coding sequence (positions 5362, 5365, 5368 and 5371). Oligonucleotides C21 and C22 were complementary to each other and contained another four nucleotide substitutions (underlined) corresponding to the N-terminus of the 3C coding sequence (positions 5440, 5443, 5446 and 5449). The four resulting PCR fragments were gel purified. Fragments 1 and 2 were mixed and used as one template, and fragments 3 and 4 were mixed and used as another template in two separate new PCRs with the primers 2910 and 2912. The final two products (474 bp) were digested with *Hpa*I–*Bgl*II to yield two 425 bp fragments, which were then inserted into the poliovirus cDNA clone pT7-PVM (Cao *et al.*, 1993) at the corresponding *Hpa*I–*Bgl*II sites. After selection and propagation in *Escherichia coli* strain DH5, the recombinant plasmids pPVM-2VPg-3 and -4 were confirmed by sequence analysis in the region of mutagenesis (Figure 1).

Construction of plasmid pPVM-2VPg-5. In order to insert an additional VPg coding sequence into the poliovirus RNA genome, where the nucleotides were partially substituted but maintained the wild-type amino acid sequences, we used a similar two-step PCR strategy. As illustrated in Figure 5A, 28 nucleotides at the 3′ end of the oligonucleotide C31 were complementary to the VPg sequences in pT7-VPg15, the remaining 41 nucleotides of the oligonucleotide C31 were complementary to the VPg sequences in pT7-VPg22 at a lower homology of 66% (GGGACATTTGGTCTTTTATTAGGAAGTCCTGTATAAGCACCTT-GTACCTTTGCGGTCCGAATGGTGGGC). The 32 nucleotides at the 3′-end of the oligonucleotide C32 were identical to the 5′-end of 3C sequences, and the remaining 36 nucleotides of the oligonucleotide C32 shared lower homology (64%) to that of the VPg sequences in pT7-VPg22 (CCAAATGTCCCAACAATCAGAACAGCTAAAGTTCAGG-GCCCCGGGTTCGATTACGCAGTGGCTATGGC). The 11 nucleotides at the 5′ end of each oligonucleotides C31 and C32 were complementary to each other.

First, two PCRs were performed using the DNA plasmid pPVM-2VPg-2 as template for extension of the primers C31 and 2910 in one reaction, and of the primers C32 and 2912 in another reaction. In the second step, the two resulting PCR fragments were gel purified and added to a new PCR as template with primers 2910 and 2912. The final product (474 bp) was digested with *HpaI–BglII* to yield a 425 bp fragment, which was then inserted into the *HpaI–BglII* region of the plasmid pT7-PVM. The new recombinant plasmid, pPVM-2VPg-5, contained two VPg coding sequences which shared 64% homology to each other at the nucleotide level (see Figure 5).

Viral RNA purification and RNA sequencing

HeLa cell monolayers were infected with viruses derived from RNA transfections at a multiplicity of infection (MOI) of 10–30. After 5–7 h post-infection, total cytoplasmic RNAs were extracted from HeLa cells as described previously (Reuer *et al.*, 1990). Sequences around the VPg region of the RNAs were sequenced by the dideoxy-chain termination method using [α-^{35}S]dATP and avian myeloblastosis virus reverse transcriptase.

Detection of intergenomic recombinant RNAs by RT/PCR

Viruses, derived from RNA co-transfections, were used to infect HeLa monolayers. Total cytoplasmic RNAs were extracted at 6 h post-infection. First strand cDNAs were synthesized using Tth-DNA polymerase (Boehringer Mannheim) and oligonucleotide 2933 (GCTGTAACAATG-TTTCTTTTAGCC, complementary to positions 5467–5490) as primer. The PCRs were performed using the cDNAs as templates and oligonucleotides C25 and C26 or C27 and C28 as primers. The sequences of these oligonucleotides are: C25 (GTTTGCAGGACATCAA), C26 (GTAATCAAAGCCTGGT), C27 (GTAATCGAACCCGGGG) and C28 (GTTTGCTGGTCACCAG). C25 and C28 were complementary to the negative strand of the poliovirus genome at positions 5356–5371; C26 and C27 were complementary to the positive strand at positions 5440–5455 (see Figure 1B). All PCR products were analysed via agarose gel electrophoresis.

In vitro translation

Viral RNAs transcribed *in vitro* from cDNA plasmids pPVM-2VPg-2, -3, -4 and -5 were mixed with a nuclease-treated HeLa cell extract (S10 fraction) in addition to translation mixture (Molla *et al.*, 1991) and 1 mCi of [^{35}S]methionine/ml. Incubations were performed at 34°C from 1.5 to 8 h. Samples were analyzed by a 10–20% gradient SDS–PAGE and subsequent autoradiography.

Pulse labeling of infected cells with [^{35}S]methionine and immunoprecipitation

HeLa cell monolayers in 60 mm Petri dishes [10^6 cells] were infected with wild-type or revertant virus isolates at an MOI of 30 in DME medium supplemented with 5% fetal bovine serum. At 4 h post-infection, cells were washed three times with methionine-free minimal essential medium and incubated in the methionine-free medium for 1 h. At 5 h post-infection, infected cells were pulse labeled with [^{35}S]methionine (45 μCi/dish; Amersham Corp.) for 5–15 min. Excess cold methionine was then added to stop the pulse labeling of proteins. The cells were continuously incubated from 0 to 60 min. At the end of the incubation, the medium was removed and the cells were washed three times with cold phosphate-buffered saline. Finally, the cells were lysed in 200 ml NP40 lysis buffer [100 mM NaCl, 0.5% NP40, 1 mM EDTA, 10 mM Tris–HCl (pH 7.5)]. Labeled viral proteins were analyzed by a 10–25% gradient SDS–PAGE.

Immunoprecipitation was performed essentially as described previously (Cao *et al.*, 1993).

Acknowledgements

We are indebted to David A.Matthews and Stephen Worland (Agouron Pharmaceuticals) for explaining to us the structural features of human rhinovirus and poliovirus 3C^{pro} proteinases, and we are grateful to our colleagues Michael Shepley and Fred Lahser for critical reading and editing of the manuscript. We thank Peter Kissel for the synthesis of oligonucleotides. This work was supported in part by Public Health Service grants A1-15122 and R01AT-32100 from the National Institutes of Health, and by HFSPO PN93297 from the Human Frontier Science Program Organization.

References

Bienz,K., Egger,D., Rasser,Y. and Bossart,W. (1980) Kinetics and location of poliovirus macromolecular synthesis in correlation to virus-induced cytopathology. *Virology*, **100**, 390–399.

Bienz,K., Egger,D., Rasser,Y. and Bossart,W. (1987) Association of polioviral protein of the P2 genomic region with the viral replication complex and virus-induced membrane synthesis as visualized by electron microscopic immunocytochemistry and autoradiography. *Virology*, **160**, 220–226.

Blair,W.S. and Semler,B.L. (1991) Role for the P4 amino acid residue in substrate utilization by the poliovirus 3CD proteinase *J. Virol.*, **65**, 6111–6123.

Cao,X.M. and Wimmer,E. (1995) Intragenomic complementation of a 3AB mutant in dicistronic polioviruses. *Virology*, **209**, 315–326.

Cao,X.M., Kuhn,R.J. and Wimmer,E. (1993) Replication of poliovirus RNA containing two VPg genes leads to a specific deletion event. *J. Virol.*, **67**, 5572–5578.

Falk,M.M., Sobrino,F. and Beck,E. (1992) VPg gene amplification correlates with infective particle formation in foot-and-mouth disease virus. *J. Virol.*, **66**, 2251–2260.

Forss,S., Strebel,K., Beck,E. and Schaller,H. (1984) Nucleotide sequence and genome organization of foot-and-mouth disease virus. *Nucleic Acids Res.*, **12**, 6587–6601.

Gmyl,A.P., Pilipenko,E.V., Maslova,S.V., Belov,G.A. and Agol,V.I. (1993) Functional and genetic plasticities of the poliovirus genome: Quasi-infectious RNAs modified in the 5′- untranslated region yield a variety of pseudorevertants. *J. Virol.*, **67**, 6309–6316.

Harris,K.S., Reddigari,S.R., Nicklin,M.J.H., Haemmerle,T. and Wimmer,E. (1992) Purification and characterization of poliovirus polypeptide 3CD, a proteinase and a precursor for RNA polymerase. *J. Virol.*, **66**, 7481–7489.

Harris,K.S., Xiang,W., Alexander,L., Paul,A.V., Lane,W.S. and Wimmer,E. (1994) Interaction of the polioviral polypeptide 3CD^{pro} with 5′ and 3′ termini of the poliovirus genome: Identification of viral and cellular cofactors necessary for efficient binding. *J. Biol. Chem.*, **269**, 27004–27014.

Holland,J.J., De La Torre,J.C. and Steinhauer,D.A. (1992) Genetic diversity of RNA viruses. *Curr. Top. Microbiol. Immunol.*, **176**, 1–20.

Jarvis,T.C. and Kirkegaard,K. (1992) Poliovirus RNA recombination: mechanistic studies in the absence of selection. *EMBO J.*, **11**, 3135–3145.

King,A.M.Q. (1988a) Recombination in positive strand RNA viruses. In *RNA Genetics*. CRC Press, Boca Raton, FL, Vol. 2, pp. 149–165.

King,A.M.Q. (1988b) Preferred sites of recombination in poliovirus RNA: an analysis of 40 intertypic cross-over sequences. *Nucleic Acids Res.*, **16**, 11705–11723.

Kirkegaard,K. and Baltimore,D. (1986) The mechanism of RNA recombination in poliovirus. *Cell*, **47**, 433–443.

Kraeusslich,H.G. and Wimmer,E. (1988) Viral proteinases. *Annu. Rev. Biochem.*, **57**, 701–754.

Kuhn,R.J. and Wimmer,E. (1987) The replication of picornaviruses. In *The Molecular Biology of Positive Strand RNA Viruses*. Academic Press, London, pp. 17–51.

Kuhn,R.J., Tada,H., Ypma-Wong,M., Dunn,J.J., Semler,B.L. and Wimmer,E. (1988) Construction of a 'mutagenesis cartridge' for poliovirus genome-linked viral protein: isolation and characterization of viable and nonviable mutants. *Proc. Natl Acad. Sci. USA*, **85**, 519–523.

Lai,M.M.C. (1992) RNA recombination in animal and plant viruses. *Annu. Rev. Microbiol.*, **56**, 61–79.

Lama,J., Paul,A.V., Harris,K.S. and Wimmer,E. (1994) Properties of purified recombinant poliovirus protein 3AB as substrate for viral proteinases and as co-factor for viral polymerase 3D^{pol}. *J. Biol. Chem.*, **269**, 66–70.

Lawson,M.A. and Semler,B.L. (1991) Poliovirus thiol proteinase 3C can utilize a serine nucleophile within the putative catalytic triad. *Proc. Natl Acad. Sci. USA*, **88**, 9919–9923.

Matthews,D.A. *et al.* (1994) Structure of human rhinovirus 3C protease reveals a trypsin-like polypeptide fold, RNA-binding site, and means for cleaving precursor polyprotein. *Cell*, **77**, 761–771.

Molla,A., Paul,A.V. and Wimmer,E. (1991) Cell-free, de novo synthesis of poliovirus. *Science*, **254**, 1647–1651.

Molla,A., Harris,K.S., Paul,A.V., Shin,S.H., Mugavero,J. and Wimmer,E. (1994) Stimulation of poliovirus proteinase 3C^{pro}-related proteolysis by the genome-linked protein VPg and its precursor 3AB. *J. Biol. Chem.*, **269**, 27015–27020.

Nicklin,M.J.H., Toyoda,H., Murray,M.G. and Wimmer,W. (1986) Proteolytic processing in the replication of polio and related viruses. *Biotechnology*, **4**, 33–42.

Pallai,P.V. *et al.* (1989) Cleavage of synthetic peptides by purified poliovirus 3C proteinase. *J. Biol. Chem.*, **264**, 9736–9741.

Reuer,Q., Kuhn,R.J. and Wimmer,E. (1990) Characterization of poliovirus clones containing lethal and nonlethal mutations in the genome-linked protein VPg. *J. Virol.*, **64**, 2967–2975.

Romanova,L.I., Blinov,V.M., Tolskaya,E.A., Viktorova,E.G., Kolesnikova,M.S., Guseva,E.A. and Agol,V.I. (1986) The primary structure of crossover regions of intertypic poliovirus recombinants: a model of recombination between RNA genomes. *Virology*, **155**, 202–213.

Semler,B.L., Anderson,C.W., Kitamura,N., Rothberg,P.G., Wishert,W.L. and Wimmer,E. (1981) Poliovirus replication proteins: RNA sequence encoding P3-lb and the site of proteolytic processing. *Proc. Natl Acad. Sci. USA*, **78**, 3464–3468.

van der Werf,S., Bradley,J., Wimmer,E., Studier,F.W. and Dunn,J.J. (1986) Synthesis of infectious poliovirus RNA by purified T7 RNA polymerase. *Proc. Natl Acad. Sci. USA*, **83**, 2330–2334.

Wimmer,E., Hellen,C.U.H. and Cao,X.M. (1993) Genetics of poliovirus. *Annu. Rev. Genet.*, **27**, 353–436.

Xiang,W., Harris,K.S., Alexander,L. and Wimmer,E. (1995) Interaction between the 5′-terminal cloverleaf and 3AB/3CD^{pro} of poliovirus is essential for RNA replication. *J. Virol.*, **69**, 3658–3667.

Ypma-Wong,M.-F., Dewalt,P.G., Johnson,V.H., Lamb,J.G. and Semler,B.L. (1988a) Protein 3CD is the major poliovirus proteinase responsible for cleavage of the P1 capsid precursor. *Virology*, **166**, 265–270.

Ypma-Wong,M.-F., Filman,D.J., Hogle,J.M. and Semler,B.L. (1988b) Structural domains of the poliovirus polyprotein are major determinants for proteolytic cleavage at Gln-Gly pairs. *J. Biol. Chem.*, **263**, 17846–17856.

Received on July 27, 1995; revised on September 15, 1995